Enhancement of Methane Formation from Methanethiol Adsorbed on a Strained Ni Film on W(001)

David R. Mullins

Oak Ridge National Laboratory, Oak Ridge, Tennessee 37831-6201

Received: October 14, 1996; In Final Form: December 10, 1996[⊗]

The selective formation of methane from the decomposition of methanethiol increases as the coverage of Ni thin films is increased from 0 to 2 monolayers (ML) on W(001). The methane selectivity starts at 30% on the clean W(001) surface, rises to 70% when the Ni coverage is 1 ML, dips to 60% at 1.5 ML, and then continues to rise to >85% when the Ni coverage is 2 ML. This is the largest selectivity for methane formation yet reported for this reaction in ultrahigh vacuum. Accompanying the increase in selectivity is a sequential decrease in the methane desorption temperature. The methane desorbs at 350 K from methanethiol on clean W(001), at 290 K from a 1 ML Ni film, and at 210 K from a 2 ML Ni film. On thick (>5 ML), unannealed films, the desorption temperature increases to 270 K and the selectivity is reduced to 70%. S 2p soft X-ray photoemission indicates that the C−S bond is cleaved between 300 and 350 K on clean W(001) and between 250 and 300 K on a 1 ML Ni film. On the 2 ML Ni film, there is considerable C−S bond cleavage (>50%) at 100 K. The only molecular intermediates are methyl thiolate (CH_3S) and hydrocarbon fragments . The methyl thiolate forms at 100 K at all Ni coverages. An amount of 65% of the thiolate occupies low coordination sites on clean W(001), while most of the thiolates occupy high coordination sites on the Ni-covered surfaces.

Introduction

The selectivity and temperature for methane formation from the decomposition of methanethiol vary widely on different metal surfaces. On W(001) only 30% of the chemisorbed thiol forms methane, which desorbs at 350 K.[1] Alternatively, 75−80% of the thiol produces methane on low-index crystal faces of pure Ni, and the methane desorption occurs at much lower temperature (270 K).[2−4] The decomposition of methanethiol falls somewhere between these two extremes on most other metal surfaces.[5−10]

Bimetallic alloys and thin films of one metal on another are known to have reactive properties that are different from either component separately.[11,12] Since Ni and W lie at the extremes of methanethiol reactivity on metals, it is of interest to explore a bimetallic system consisting of these two components. In addition, Ni serves as a promoter for WS_2 desulfurization catalysts.[13] Ni/W is therefore a logical choice for investigating the behavior of methanethiol on a bimetallic surface.

To relate the structure and composition of the bimetallic surface to the reactive properties of methanethiol, the structure of the surface needs to be well characterized. Ni on W(001) has been shown to grow in a Stransky−Krastinov, or layer by layer, manner for coverages up to 2 monolayers (ML) (2×10^{15} cm^{-2}).[14] For coverages less than 1 ML, mixing, or surface alloy formation, occurs between the W and the Ni when the sample is annealed above 700 K. However, at 1 ML the Ni overlayer forms a homogeneous pseudomorphic layer. Between 1 and 2 ML mixing again occurs at the Ni−W interface, but at 2 ML the Ni forms two homogeneous pseudomorphic layers. The structure at Ni coverages above 2 ML is uncertain but does depend on whether the sample is annealed. A film grown at room temperature seems to continue to grow layer by layer but with an unknown structure. If the sample is annealed above 800 K, the Ni clusters into three-dimensional islands. A major issue addressed in the current investigation is the behavior of methanethiol on W(001) with small Ni coverages, where the thiol can interact with both Ni and W, compared to the behavior on large Ni coverages, where the thiol is only able to interact with the strained Ni layer.

The only published report of the decomposition of methanethiol on a bimetallic surface is CH_3SH on Co-covered Mo(110).[15] In that study, Chen et al. reported that for Co coverages up to 1 ML, the selectivity and desorption temperature of CH_3/CH_4 do not change significantly. The main difference between the clean and Co-covered Mo(110) surfaces is that on the clean Mo surface there is a substantial amount of methyl radical desorbed, whereas on the Co-covered surface CH_4 desorbs instead of CH_3.

Conversely, there are substantial changes in the selectivity and reaction kinetics of the decomposition of methanethiol as a function of Ni coverage on W(001). The present study shows that the formation of methane increases dramatically for Ni coverages up to 2 ML. This increase is accompanied by a decrease in the methane desorption temperature. At 2 ML of Ni, >85% of the adsorbed thiol produces methane and substantial C−S bond cleavage is indicated at temperatures as low as 100 K.

Experimental Section

The experimental system and sample preparation have been described in detail previously.[1,14] The crystal was cleaned by repeated cycles of annealing in oxygen to remove surface and near-surface carbon followed by flashing to approximately 2300 K to remove surface oxygen. Nickel films were vapor deposited from a Ni wire wrapped around a W filament. Depositions were done with the W(001) sample at 100 K and then annealed to 1000 K unless otherwise indicated. Impurity and Ni coverages were determined from Auger electron spectroscopy (AES), and the Ni coverage was calibrated as described previously using a change in the Ni/W AES intensity ratio induced by heating, which occurs above 2 ML.[14,16] AES measurements of Ni

[⊗] Abstract published in *Advance ACS Abstracts,* January 15, 1997.

S1089-5647(96)03150-1 CCC: $14.00

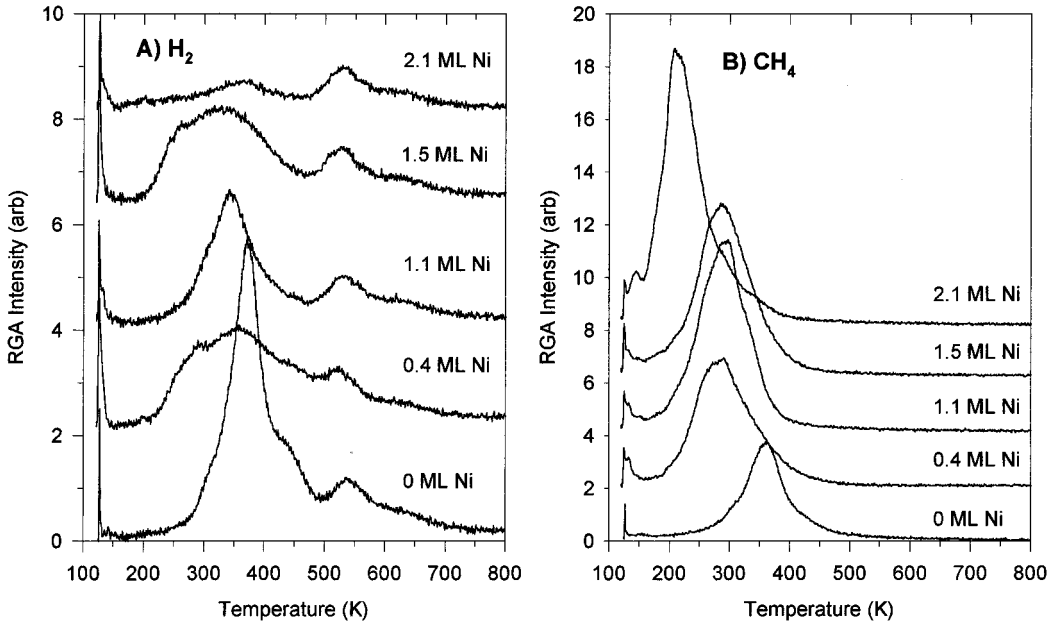

Figure 1. Desorption spectra of hydrogen (A) and methane (B) from a multilayer of CH_3SH adsorb on W(001) covered with various amounts of Ni.

coverage were also correlated with the Ni temperature-programmed desorption intensity.

Methanethiol exposures were made through a directed doser[1] after the metal substrate had cooled to 100 K. CH_3SH (Matheson,99.5%) and CH_3SD (MSD) were purified by several freeze/pump/thaw cycles and the purity checked by the mass spectrometer. The isotopic purity of the CH_3SD was estimated to be 70% based on the mass spectrometer cracking pattern. AES and S 2p photoemission were used to determine the amount of CH_3SH that decomposed on the surface. It was previously determined that 0.6 ML of CH_3SH irreversibly adsorbs on the clean W(001) surface.[1] The sample was resistively heated for the thermal desorption experiments and was biased at −70 V to minimize electron-stimulated reactions that could be induced by current from the ionizer of the residual gas analyzer (RGA).[8,17]

The photoemission spectra were recorded on the U13UA beamline at the National Synchrotron Light Source unless otherwise indicated. Excitation energies of 250 and 380 eV were used for the S 2p and the C 1s spectra, respectively. The total instrumental resolution was estimated to be 0.30 eV. The spectra were referenced against the bulk W $4f_{7/2}$ peak at 31.42 eV.[14] The emission angle was 15° from the surface normal. This emission angle minimized diffraction effects and gave the most reliable S 2p intensities for determining the partial coverages of different S-containing species. This was evident in the fact that the total S 2p intensity remained constant as the sample was heated and the thiolate decomposed. The spectra were normalized to the background intensity at kinetic energies slightly higher (1−2 eV) than the S 2p or C 1s signals.

Results

Thermal Desorption. The desorption of H_2, CH_4, and CH_3SH were recorded at mass 2, 16, and 48, respectively. It was previously established that no other desorption products occur from the clean W(001) surface.[1] In particular, C_2H_4 at mass 28, C_2H_6 at mass 30, H_2S at mass 34, and $(CH_3S)_2$ at mass 94 were not detected. In addition, a comparison of the line shapes and the relative intensities of mass 15 and mass 16 desorbing from the clean W(001) surface indicated that CH_3 was also not a major desorption product. The balance between the H_2 and CH_4 intensities and the amount of S left on the surface indicated that these two species were the only desorption products from the Ni-covered surface as well.

The H_2 and CH_4 desorption spectra from a multilayer exposure of CH_3SH on W(001) with various coverages of Ni are shown in parts A and B of Figure 1, respectively. On the Ni-free surface, H_2 desorbs in an intense peak near 370 K with a shoulder between 400 and 450 K. The peak at 525 K is from residual H_2 that adsorbed on the back of the crystal.[1] When Ni is preadsorbed on the W surface, the H_2 desorption intensity is reduced and the main desorption feature is shifted down to ca. 350 K. With 0.4 and 1.5 ML of preadsorbed Ni, the spectra are broadened toward lower temperatures with an onset near 200 K. This broadening disappears at 1 ML of Ni. Above 2 ML of Ni, the H_2 desorption intensity becomes very weak with only a small peak apparent near 370 K. The peak at 525 K remains at the same intensity at all Ni coverages.

CH_4 desorbs in a single peak near 350 K on the Ni-free surface (Figure 1B). As the Ni coverage is increased, the desorption peak shifts down to 290 K and the integrated intensity increases. Near 2 ML of Ni, the peak shifts down to 210 K.

The selectivity for H_2 and CH_4 formation from the decomposition of CH_3SH on W(001) as a function of Ni coverage is shown in Figure 2. The selectivity is defined as the fraction of CH_3SH that decomposes into a given product. The amount of CH_3SH that decomposes remains constant at 0.6 ML ± 10%. On the Ni-free surface, one-third of the thiol selectively decomposes producing CH_4 and two-thirds totally decomposes producing H_2.[1] As the Ni coverage increases, the fraction producing CH_4 rises and the fraction producing H_2 decreases. At 1 ML of Ni the selectivities along the two paths are reversed with roughly two-thirds resulting in CH_4 and one-third producing H_2. Above 1 ML of Ni the selectivity for methane formation dips to ca. 0.60 and then continues to increase and levels off at ca. 0.85 near a Ni coverage of 2 ML. For films annealed to 1000 K before thiol adsorption, the selectivities remain constant for Ni thicknesses above 5 ML. If the film is not annealed (open symbols in Figure 2), the CH_4 yield drops to <0.75 for thick Ni films.

Hydrogen and methane desorption spectra from CH_3SD adsorbed on W(001) at various Ni coverages are shown in Figure

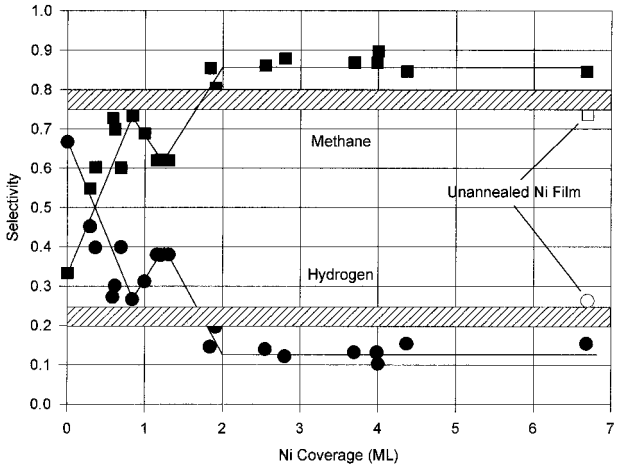

Figure 2. Selectivity (see text) for methane (■) and hydrogen (●) formation during the decomposition of a multilayer of CH_3SH on Ni-covered W(001) as a function of Ni coverage. All the Ni films were annealed to 1000 K before exposure to CH_3SH except for the points indicated (□ and ○). The striped bands indicate the selectivity on the three low-index crystal faces of pure Ni.[2−4]

3. The figure is intended to qualitatively indicate how the sulfhydryl hydrogen from the methanethiol is incorporated into the desorption products. H_2, HD, CH_4, and CH_3D were monitored at mass 2, 3, 15, and 17, respectively. An amount of 20% of the CH_3D signal observed at mass 17 overlaps with the CH_4 signal at mass 15.[18] The CH_4 spectra shown in Figure 3 have been corrected accordingly. No attempt was made to correct for isotopic purity. D_2 (mass 4) desorption was also recorded. The qualitative trends observed in the HD desorption also occur in the D_2 desorption, so the D_2 spectra have been omitted for clarity. The mass 15 and mass 2 peaks below 150 K are the result of methanethiol-cracking fragments.

On the Ni-free surface there is a large fraction of HD desorbed. The HD desorption reaches a maximum at a slightly lower temperature than the H_2, and there is no deuterium incorporation above 400 K. The CH_4 and CH_3D start desorbing at the same temperature. However, there is again no deuterium incorporation above 400 K. The intensity of the CH_4 desorption is larger than the intensity of the CH_3D desorption. On the 0.5 ML Ni film, the H_2 and HD desorptions are more clearly separated with the HD desorbing primarily between 250 and 350 K and the H_2 desorbing above 350 K. The CH_3D intensity is slightly greater than the CH_4 intensity, and both peaks shift to 290 K. The HD desorption peak shifts back to 350 K on 1 ML of Ni and slightly precedes the H_2 desorption. The CH_3D fraction continues to increase but the desorption temperature remains at 290 K. The CH_4 desorption has a slightly higher peak temperature. At 1.5 ML of Ni the HD desorption again shifts to lower temperatures relative to the H_2 desorption. The CH_3D desorbs at a lower temperature than the CH_4. However, the integrated intensity in the two masses is about the same. Finally, the HD desorption is nearly gone on the 2 ML Ni film and CH_3D dominates the methane desorption spectra. Both CH_3D and CH_4 shift down to 210 K.

H_2 and CH_4 produced by CH_3SH decomposition on W(001) with a Ni coverage greater than 5 ML are shown in Figure 4. H_2 desorption from a sample annealed to 1000 K before thiol adsorption is similar to desorption from a 2 ML film, although the H_2 desorption stretches from 200 to 400 K and is somewhat more intense than on the 2 ML film. The CH_4 desorption is complex, although it still shows a prominent peak at 210 K as well as peaks at 240 and 270 K. On an unannealed multilayer Ni film, two prominent H_2 desorption peaks are seen at 250 and 320 K as well as the peak from the back of the sample at 500 K. The increased intensity above 500 K reflects the amount of time the sample sat in the ambient environment while the Ni film was deposited and then not annealed to remove the hydrogen that adsorbed from the background. CH_4 desorbs from the unannealed film in a single, symmetric peak at 270 K.

S 2p Photoemission. S 2p photoemission spectra from CH_3SH adsorbed on 0, 1, and 2 ML of Ni on W(001) and annealed as indicated are shown in Figures 5−7, respectively. Spectra are shown for both a low thiol exposure, 0.2 ML, and a saturation exposure, >0.6 ML. The S $2p_{3/2}$ peak positions are indicated in the low-coverage spectra and are assigned labels, ${}^{\#}S_L$, where # is the Ni coverage and L is an alphabetical index that runs from lowest to highest binding energy. The S $2p_{3/2}$ peak positions and their assignments are summarized in Table 1.

S 2p photoemission spectra from CH_3SH on clean W(001) are shown in Figure 5 and are the same as have been presented previously.[1,19] The spectra in Figure 5A were obtained on beamline U3C using an excitation energy of 210 eV and have an instrumental resolution of 0.5 eV. Two S 2p states are seen upon adsorption at 100 K. ${}^0S_C$, at 163.7 eV, has been assigned to CH_3S in a 4-fold site[1] and is the most intense state at low coverage (Figure 5A). ${}^0S_A$, at 162.55 eV, has been assigned to CH_3S in a bridge or a top site and becomes twice as intense as ${}^0S_C$ when the coverage is increased to 0.6 ML (Figure 5B). As the 0.2 ML CH_3SH is annealed, the initial S 2p states decrease in intensity at 250 K and a new state, ${}^0S_B$, emerges at 163.05 eV and is assigned to atomic S in a 4-fold site. The original states disappear by 350 K and the spectrum is unchanged as the sample is annealed to higher temperatures. Physisorbed CH_3SH, ${}^0S_D$, is seen at 100 K in Figure 5B at a binding energy of 164.5 eV (which is more obvious in the $2p_{1/2}$ component at 165.7 eV) . After the physisorbed thiol desorbs below 150 K, the spectra from 0.6 ML of CH_3SH remain essentially unchanged up to 300 K. At 350 K, ${}^0S_C$ disappears (this can be seen most clearly in the disappearance of the S $2p_{1/2}$ component near 164.9 eV). New states appear near 162 and 163 eV. At 1000 K the S 2p states shift to much lower binding energy. This shift is caused by a surface reconstruction.[1,19]

S 2p spectra from 0.2 and >0.6 ML of CH_3SH on W(001) covered with 1 ML of Ni are shown in parts A and B of Figure 6, respectively. At 100 K the S 2p signal from 0.2 ML of CH_3SH is concentrated in a single state, ${}^1S_C$, near 163.0 eV. A very small state, ${}^1S_B$, can be seen near 162.3 eV. As the sample is heated, ${}^1S_C$ decreases in intensity and a new peak, ${}^1S_A$, appears at 161.9 eV. The spectra do not change significantly above 300 K. In the spectra from >0.6 ML of CH_3SH, physisorbed thiol again desorbs between 100 and 150 K and the spectra are then unchanged up to 200 K. ${}^1S_C$ is more than twice as intense as ${}^1S_B$. At 250 K a shoulder appears on the low binding energy side of ${}^1S_B$. By 300 K this shoulder has grown into ${}^1S_A$ and the higher binding energy states decrease in intensity. Only ${}^1S_A$ is evident at 350 K. At 1000 K a shoulder appears at 161.4 eV.

S 2p spectra from 0.2 and 0.6 ML of CH_3SH on W(001) covered with 2 ML of Ni are shown in parts A and B of Figure 7, respectively. Three states are evident in the spectrum from 0.2 ML of CH_3SH at 100 K. The most intense state, ${}^2S_A$, is at 162.2 eV, and two smaller states with nearly equal intensity, ${}^2S_B$ and ${}^2S_C$, occur at 162.7 and 164.3 eV, respectively. The higher binding energy states decrease in intensity at 150 K and are gone by 200 K. The spectra are then unchanged upon further annealing. The greatest intensity in the spectrum from 0.6 ML of CH_3SH at 100 K is from CH_3SH at binding energies greater than 164 eV. The CH_3SH signal mostly disappears at 150 K.

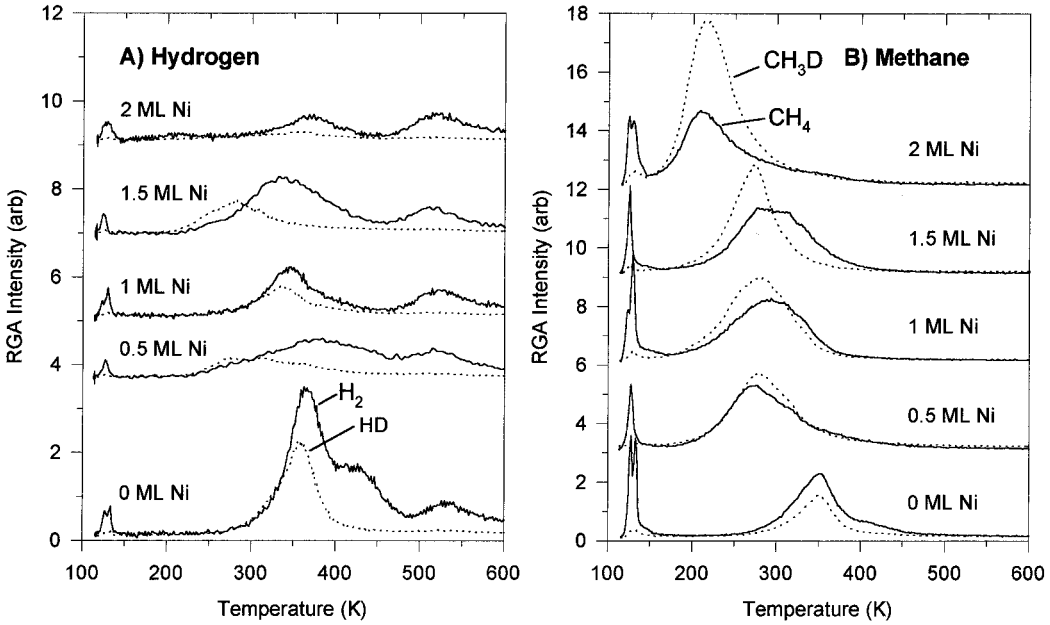

Figure 3. Desorption spectra of hydrogen (A) and methane (B) during the decomposition of CH_3SD on various coverages of Ni on W(001). The solid lines indicate the nondeuterated products, H_2 or CH_4, and the dotted lines indicate the deuterated products, HD and CH_3D.

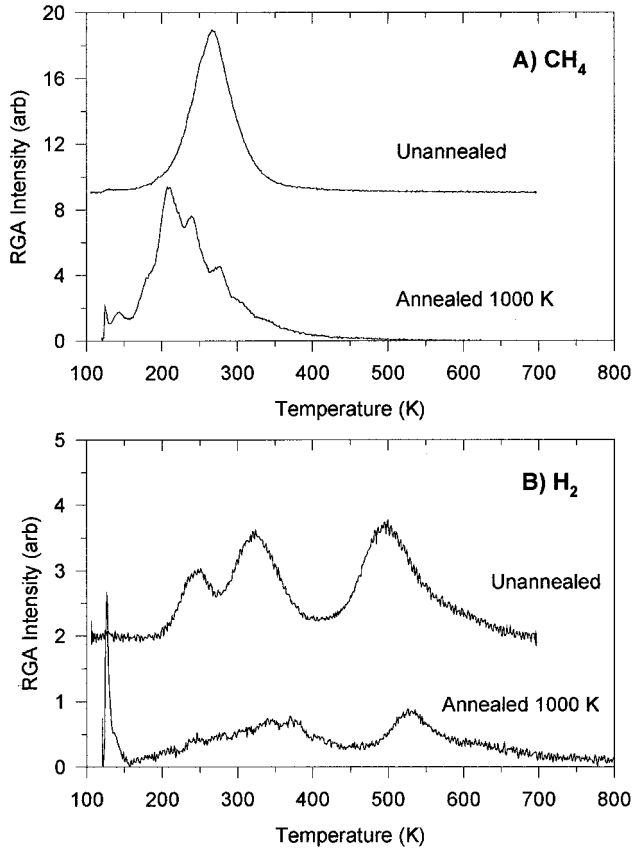

Figure 4. Desorption spectra of methane (A) and hydrogen (B) from thick (>5 ML) Ni films on W(001). The top curve in each panel is from an unannealed film, and the bottom curve is from a film annealed to 1000 K.

The spectrum at 150 K is quite broad. However, it appears to consist of the easily identifiable ^2S_A peak at 162.2 eV as well as unresolved intensity between 162.7 and 163 eV. At 200 K the spectrum is made up primarily of ^2S_A with a small amount of intensity at 162.5 eV. By 250 K the S 2p signal is concentrated in ^2S_A. As the sample is heated further, the spectra sharpen and well-defined states split off at lower binding energies.

TABLE 1: S $2p_{3/2}$ Peak Positions and Adsorption Site Assignments

label	binding energy (eV)	assignment
^0S_A	162.55	CH_3S in W(001) bridge site
^0S_B	163.00	atomic S in W(001) 4-fold site
^0S_C	163.70	CH_3S in W(001) 4-fold site
^0S_D	164.50	physisorbed CH_3SH
^1S_A	161.95	atomic S in 4-fold site on 1 ML Ni
^1S_B	162.30	CH_3S in bridge site on 1 ML Ni
^1S_C	163.00	CH_3S in 4-fold site on 1 ML Ni
^2S_A	162.25	atomic S in 4-fold site on 2 ML Ni
^2S_B	162.75	CH_3S in 4-fold site on 2 ML Ni
^2S_C	164.25	CH_3SH on 2 ML Ni
	161.55	atomic S in 4-fold site on Ni(001)
	163.35	CH_3S in 4-fold site on Ni(001)

C 1s Photoemission. C 1s photoemission spectra from >0.6 ML of CH_3SH adsorbed on W(001) with 0, 1, and 2 ML of Ni are shown in Figures 8−10, respectively. On the Ni-free surface, two peaks can be seen following a 1 ML exposure of CH_3SH at 100 K. The largest peak is at 284.7 eV. This feature starts growing from the lowest exposures of CH_3SH and then saturates at 0.6 ML. The other peak at 286.2 eV starts after the first saturates and continues to grow with larger exposures. The peak at 286.2 eV disappears following an anneal at 150 K. There is a very small feature evident at 283.2 eV after the sample is annealed to 250 K. The intensity of the 284.7 eV peak decreases by ca. 15% at 300 K and by >60% at 350 K. The peak at 283.2 eV peak becomes prominent at 350 K. At 1000 K only the 283.2 eV peak remains.[20]

C 1s spectra from 1 ML of CH_3SH adsorbed on W(001) with 1 ML of Ni are shown in Figure 9. The spectra are similar to the C 1s spectra of CH_3SH on the Ni-free surface. The two peaks at 100 K are less well resolved. The poorer resolution is due to a shift of the lower binding energy peak up to 284.9 and of the higher binding energy peak down to 286.0. All of the higher binding energy state is gone at 150 K. At 250 K, the 284.9 eV peak decreases in intensity by ca. 25%, but there is only a small peak evident at 283.2 eV. At 300 K the intensity of the peak at 284.9 eV decreases by 70% compared to the intensity at 150 K. The peak at 283.2 eV grows only slightly. At 350 K only the lowest binding energy peak remains.

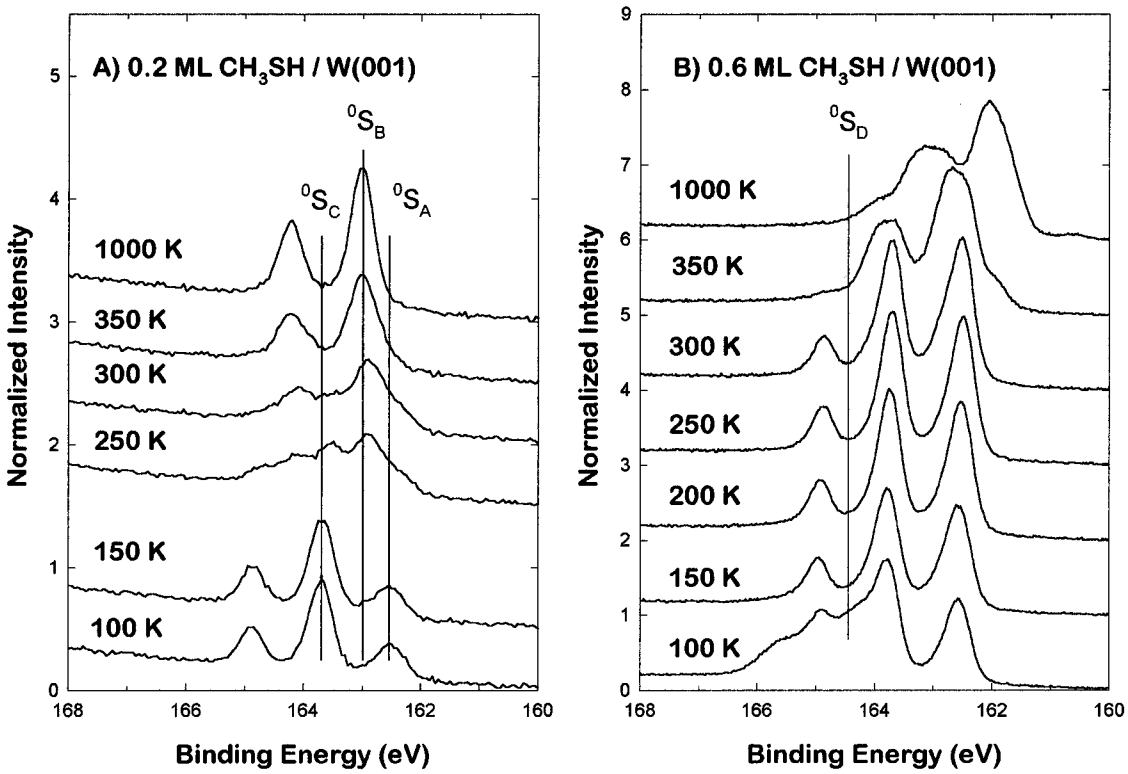

Figure 5. S 2p photoemission spectra for 0.2 (A) and 0.6 ML (B) of CH_3SH on W(001) after annealing to the indicated temperatures for 60 s.

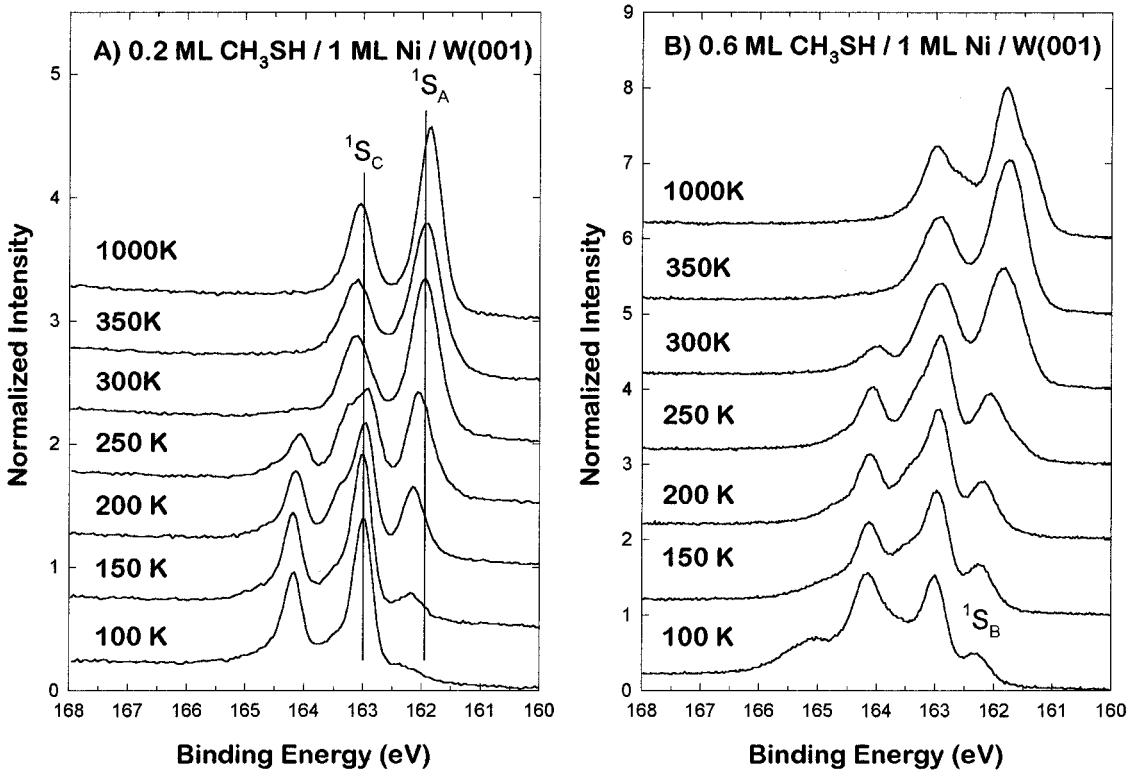

Figure 6. S 2p photoemission spectra for 0.2 (A) and 0.6 ML (B) of CH_3SH on W(001) covered with 1 ML of Ni after annealing to the indicated temperatures for 60 s.

On the 2 ML Ni film, spectra are shown at 0.2, 0.4, and 0.8 ML of CH_3SH at 100 K, as well as spectra from 0.8 ML of CH_3SH annealed to higher temperatures. At the lowest exposure, only a peak at 283.4 eV is seen. At 0.4 ML, a peak appears at 284.7 eV and then a shoulder develops near 285.9 eV following a 0.8 ML exposure. At 150 K most of the highest binding energy state disappears. However, there is still a shoulder evident near 285.5 eV. There is no change in the other two peaks. At 250 K the C 1s peaks at 283.4 and 284.7 eV are smaller and the total intensity in both peaks is $<20\%$ of what it was at 150 K. At 300 K the only C 1s signal evident is at 283.2 eV.

Discussion

The decomposition of CH_3SH on Ni-covered W(001) shows a dramatic increase in the formation of CH_4 compared to the

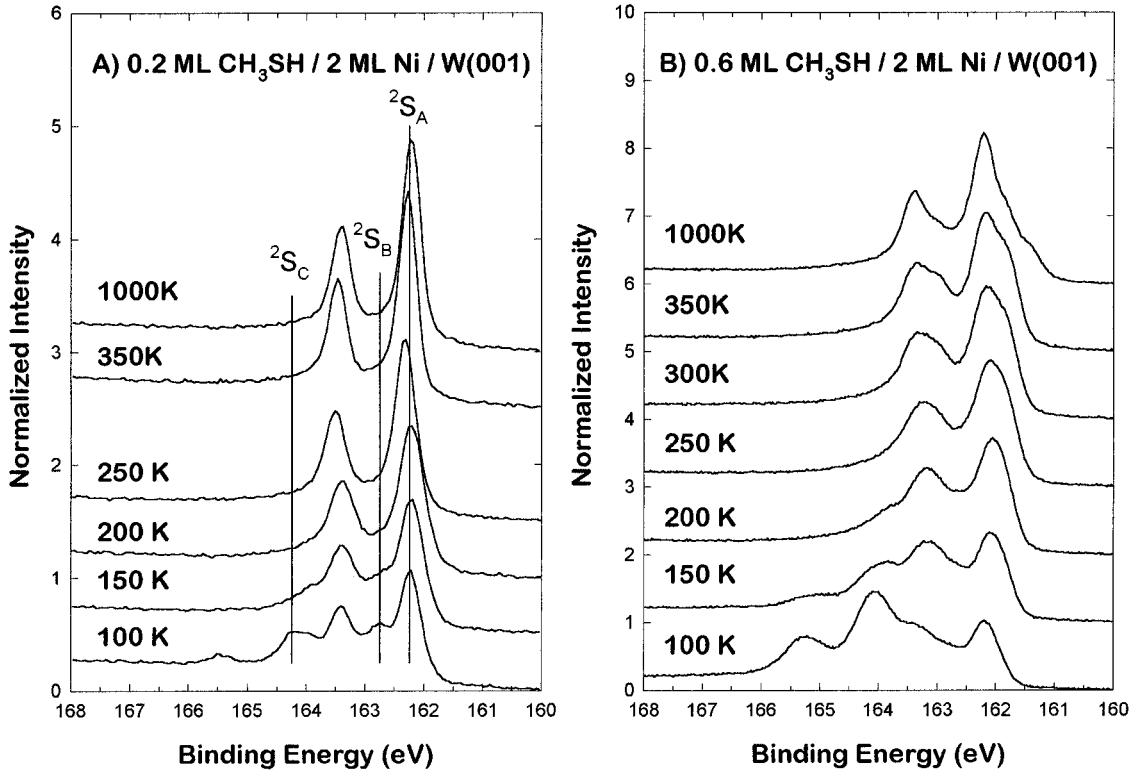

Figure 7. S 2p photoemission spectra for 0.2 (A) and 0.6 ML (B) of CH_3SH on W(001) covered with 2 ML of Ni after annealing to the indicated temperatures for 60 s.

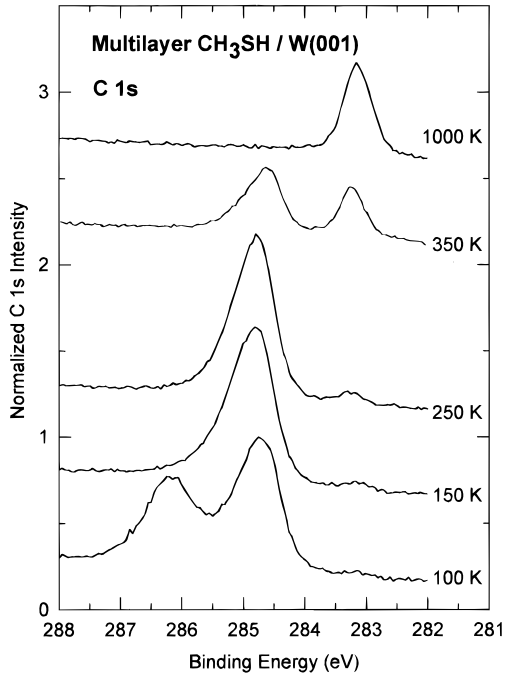

Figure 8. C 1s photoemission spectra for a multilayer of CH_3SH on W(001) after annealing to the indicated temperatures for 60 s.

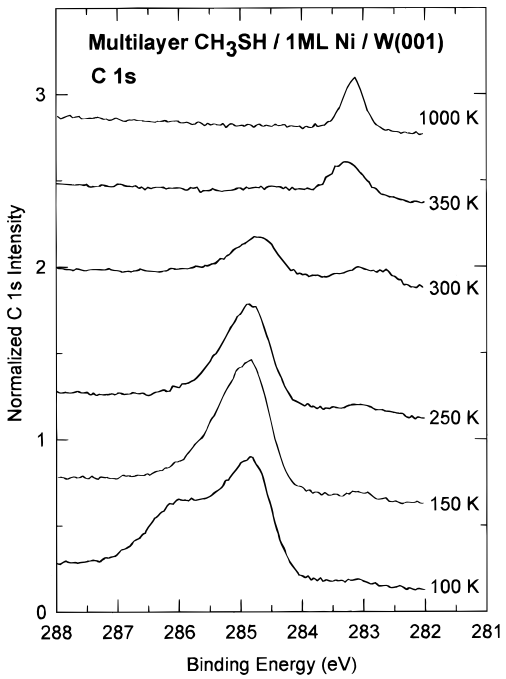

Figure 9. C 1s photoemission spectra for a multilayer of CH_3SH on W(001) covered with 1 ML of Ni after annealing to the indicated temperatures for 60 s.

decomposition of CH_3SH on a Ni-free surface. The increase in CH_4 selectivity rises with Ni coverage and reaches a maximum when the Ni coverage is 2 ML. The amount of CH_3SH that irreversibly adsorbs is unaffected by the presence of Ni. Accompanying this increase in CH_4 formation is a decrease in the CH_4 desorption temperature. The CH_4 desorption temperature decreases in discrete steps. The desorption temperature shifts from 350 K on the clean surface to 290 K on Ni coverages between 0.2 and 1.7 ML and then down to 210 K at coverages above 1.8 ML.

The increase in CH_4 selectivity is consistent with a proposal made by Wigand and Friend[9] that the selectivity will increase as the CH_4 desorption temperature decreases. This is because the methane formation reaction is then able to compete more effectively with the H_2 desorption (provided the H_2 desorption temperature does not decrease as well). In addition, methane formation also has to compete with CH_3 decomposition. The deuterium incorporation data in Figure 3 further supports this view. When no Ni is present, the CH_4 and H_2 desorption temperatures are very similar. There is a considerable amount

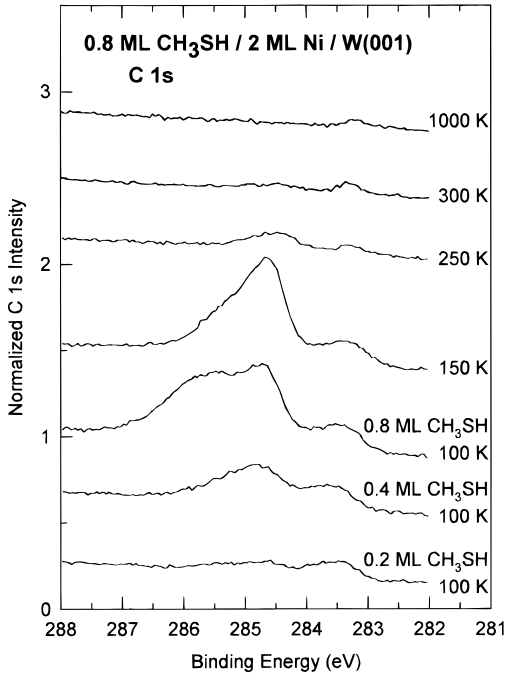

Figure 10. C 1s photoemission spectra for a multilayer of CH_3SH on W(001) covered with 2 ML of Ni after annealing to various temperatures. The bottom two curves are from submonolayer exposures of CH_3SH at 100 K.

of deuterium incorporated into the desorbing dihydrogen. This demonstrates that some of the sulfhydryl hydrogen that is adsorbed on the surface upon adsorption of CH_3SD at 100 K recombines with other surface H/D atoms rather than reacting with CH_3 to form methane. The large amount of CH_4 formed indicates that H from CH_3 decomposition is being incorporated in the desorbing methane. On the surface with 0.5 ML of Ni, the methane desorption temperature decreases but so does the hydrogen desorption temperature (Figure 1 A). The decrease in the methane desorption temperature indicates that the kinetics for methane formation are faster than the kinetics for hydrogen desorption and CH_3 decomposition, but methane formation is still far from being the exclusive reaction pathway.

When the Ni coverage is 1 ML, the temperature of the CH_4 desorption does not change significantly. However, the onset temperature for the H_2 desorption increases. The increase in the H_2 desorption temperature allows more of the surface hydrogen that came from the sulfhydryl hydrogen to be incorporated into the methane. The reduction of the hydrogen desorption temperature at submonolayer Ni coverages followed by an increase in the desorption temperature near 1 ML of Ni is reminiscent of the desorption behavior of H_2 adsorbed on Ni-covered W(001).[16]

The hydrogen desorption temperature again decreases between 1 and 2 ML. A corresponding dip from 70% to 60% occurs in the methane selectivity (Figure 2). Deuterium is again incorporated in the low-temperature hydrogen desorption.

Finally, on the 2 ML Ni film, the CH_4 desorption drops to 210 K, and essentially all the deuterium is incorporated into the CH_3D . The methane selectivity rises rapidly from ca. 60% to >85%. The small amount of hydrogen that desorbs near 350 K may be due to hydrogen adsorbed on the sample from the ambient environment. The intensity at 350 K is similar to the intensity at 525 K, which is from H_2 adsorbed on the back of the sample.

The desorption of CH_4 and H_2 from thick films (Figure 4) provides qualitative evidence of the structure of these films both before and after annealing. On an unannealed thick film, the

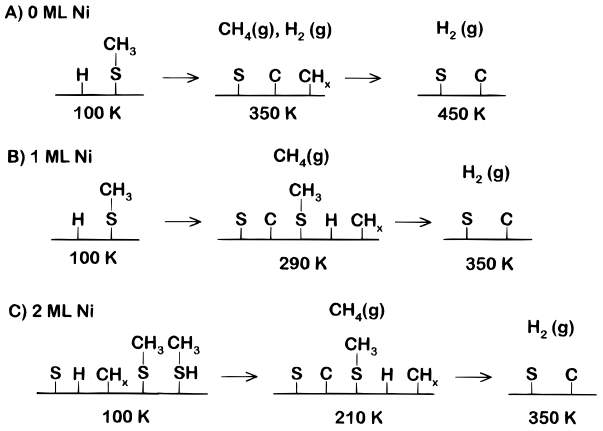

Figure 11. Reaction pathways for 0.6 ML of CH_3SH adsorbed on (A) clean W(001), (B) 1 ML Ni/W(001), and (C) 2 ML Ni/W(001) at 100 K and then heated as indicated.

methane desorbs in a single sharp peak near 270 K. The methane selectivity is near 70%. These values are very similar to what has been observed on the three low-index faces of Ni.[2−4] The H_2 desorption shows two intense peaks at 240 and 320 K as well as a large peak at 500 K from the back of the crystal. The H_2 desorption peaks are similar to the two peaks at 220 and 330 K that were observed from CH_3SH decomposition on Ni(100).[2] The hydrogen desorption behavior suggests that the structure of the unannealed film is similar to that of Ni(100). The CH_4 and H_2 desorptions from the thick, annealed films are not much different from what is observed on the 2 ML Ni film. The principal difference is a broader CH_4 desorption with identifiable peaks at 210, 240, and 275 K. These peaks imply that the annealed film consists of an exposed surface with only 2 ML of Ni as well as islands of coalesced Ni with a more bulk-like Ni structure.

S 2p and C 1s photoemission, combined with CH_3SD temperature-programmed desorption (TPD), was used to identify the reaction intermediates on the various surfaces and to study their temperature dependencies. The reaction pathways are summarized in Figure 11. The following rationale was used in assigning the observed S 2p photoemission features. Where possible, an assignment was corroborated using another technique. So, for example, the ${}^0S_B$, ${}^1S_A$, and ${}^2S_A$ states were identified by ion scattering as atomic S in 4-fold sites on 0, 1, and 2 ML Ni films, respectively.[21] The adsorption sites of atomic S and CH_3S on Ni(100) were determined by photoelectron diffraction.[22] The binding energy of CH_3S is higher than the binding energy of atomic S in the same adsorption site.[1,8,22,23] In addition, the S 2p binding energy of a species increases as the coordination of its adsorption site increases.[23] If the differentiation between CH_3S in a low-coordination site and atomic S in a high-coordination site is ambiguous, it is assumed that if C−S bond scission is going to occur at 100 K, it will happen at low thiol exposures first. Therefore, if a high binding energy state is populated first at low thiol exposures followed by a low binding energy state at higher exposures, both states are assigned to CH_3S in different adsorption sites. Finally, assignments are easier to make at lower thiol coverages because higher S coverages have been shown to cause shifts in the S 2p signals and to reconstruct the W(001) surface leading to many overlapping S 2p states.[24]

The S 2p photoemission from CH_3SH on Ni-free W(001) has been discussed previously.[1] Two states, ${}^0S_C$ and ${}^0S_A$, are seen at all thiol exposures (Figure 5). These states are assigned to CH_3S in 4-fold and bridge sites, respectively. Adsorption in the 4-fold site is favored at low exposures. However, at the

saturation coverage of CH_3S there is nearly twice as much thiolate in the bridge site as there is in the 4-fold site. As the sample is annealed, the two thiolate species decompose forming atomic S in a 4-fold site, ^0S_B. The thiolate in the 4-fold site is less stable and decomposes to a greater extent at lower temperatures than the thiolate in the bridge site. At greater thiol exposures, the onset of atomic S formation coincides with the desorption temperature of CH_4.

Two CH_3S states are also identified on the surface with 1 ML of Ni (Figure 6). At low thiol exposures nearly all of the S 2p signal is concentrated in the ^1S_C state. At higher coverages a second state, ^1S_B, is observed at lower binding energies. These states are again assigned to CH_3S in 4-fold and bridge sites, respectively. The thiolates are now bonded to Ni, however. The S 2p peak positions for both of these states are shifted to lower binding energies compared to CH_3S in the same two sites on the Ni-free surface. This shift moves the peak positions closer to what is observed for CH_3S on Ni(001) and is also in the same direction as the shift observed for atomic S on the Ni-free and 1 ML of Ni surfaces.[21] There is some ambiguity in assigning ^1S_B to CH_3S in a bridge site rather than to atomic S. However, this assignment is supported by the following observations. The binding energy of ^1S_B is different from what was previously determined for atomic S on a 1 ML Ni film.[21] The peak position shifts from 162.3 to 161.95 when atomic S is formed during decomposition. ^1S_B appears after ^1S_C and increases as the coverage increases.

There is very little C−S bond scission evident at 100 K even at low thiol exposures. Atomic S, ^1S_A, is formed at higher temperatures. At the saturation coverage of thiolate, the greatest change in the S 2p spectra occurs between 250 and 300 K, which again coincides with the desorption of CH_4. The main differences between the Ni-free and the 1 ML Ni surfaces are the predominance of the species in the 4-fold site; the lower decomposition temperature of the thiolate and the switch in the relative positions of the atomic S and the bridge-bonded thiolate states, i.e., the atomic S state occurred between the two thiolate states on the Ni-free W(001) surface.

There is considerable C−S bond scission at 100 K on the W(001) surface with 2 ML of Ni (Figure 7). There is again ambiguity in assigning the lowest binding energy state in the S 2p spectra at 100 K. In this case, ^2S_A is assigned to atomic S rather than to CH_3S in a bridge site. Unlike what was observed on the 1 ML Ni film, the binding energy of ^2S_A is the same as was previously determined for atomic S on a 2 ML Ni film.[21] The peak position does not shift and the intensity increases as the temperature is increased, which is consistent with an increase in atomic S as decomposition continues at higher temperatures. ^2S_A appears first at low exposures followed by states at higher binding energy at higher coverages, indicating that C−S bond scission is inhibited as adsorbates begin occupying the surface, and there is evidence in the C 1s data (see below) of total decomposition at low exposures, which means that one of the S 2p states at 100 K must correspond to atomic S. The binding energy of ^2S_B is midway between the binding energies assigned to 4-fold and bridge-bonded thiolates on the 1 ML film. However, CH_3S bonds only in the hollow sites on Ni(001)[22] and Ni(111)[23] and bonds predominantly in the hollow site on the 1 ML film. The trend toward bonding in hollow sites on thicker, or bulk, Ni substrates suggests assigning ^2S_B to CH_3S in the 4-fold site.

The C1s spectra are consistent with the conclusions drawn from the S 2p spectra. The C 1s peaks at highest and lowest binding energies correspond to CH_3SH and C, respectively. The high binding energy peak appears at only large CH_3SH exposures. It continues to grow as the exposure increases, and it disappears when the sample is annealed to 150 K. The exception to these observations is the 285.9 eV peak on the 2 ML Ni film. This peak appears at lower thiol exposures, and some of it persists above 150 K. This is consistent with the behavior of the ^2S_C state in the S 2p spectra. The C 1s and S 2p data indicate that the S−H bond is more stable on the 2 ML Ni film.

The peak at intermediate binding energies, 284.7−284.9 eV, is assigned primarily to CH_3S, and the peak position is not sensitive to the adsorption site of the thiolate. This assignment is consistent with the S 2p spectra from the 0 and 1 ML Ni films, where there is no indication of CH_3SH or C−S bond cleavage at 150 K. However, on the 2 ML film the S 2p spectra indicate substantial C−S bond cleavage at 100 K, yet the C 1s spectrum shows only a small amount of atomic C at 283.4 eV and a large peak at 284.7 eV. The integrated C 1s intensity indicates that there is little or no C lost through CH_4 desorption at 100 K. The conclusion is that the CH_X produced following C−S bond scission cannot be distinguished from CH_3S in the C 1s spectra. A similar conclusion was reached in previous studies of CH_3SH on clean[1] and C-covered W(001).[19] The disappearance of the atomic C peak as the sample is heated is probably due to the absorption of the C into the bulk.

The maximum selectivity for methane formation and the lowest C−S bond cleavage temperature are seen on the homogeneous film that is 2 ML thick. The maximum effect is therefore not the result of small amounts of Ni altering the W(001) surface either through site blocking or electronic perturbations. Mixing between the Ni and W actually reduces the selectivity for methane formation as seen at 1.5 ML of Ni in Figure 2. A better approach for interpreting these results is to consider how the W(001) substrate influences the properties of the Ni film.

The 2 ML of Ni film has several unique characteristics that may help explain why it exhibits such a high selectivity for methane formation. Superficially, 2 ML of Ni on W(001) appears structurally similar to the Ni(001) surface. The film has a 4-fold symmetry, and each hollow site has a Ni atom directly beneath it in the second layer. However, the film is very strained compared to Ni(001) being expanded by 27% in both orthogonal directions in the top layer and contracted by 38% between the first and second layers.[14] The more open surface with access for the reactants to the Ni in the second layer may facilitate the C−S bond cleavage.

There is also a change in the electronic strucure near the Fermi level. Photoemission spectra near the Fermi edge are shown in Figure 12 for various coverages of Ni on W(001). These spectra were recorded on the U12B beamline and have an instrumental resolution of 0.10 eV. Two effects are evident. As the Ni coverage increases, there is a decrease in intensity at the Fermi level. In addition, a pronounced peak grows at higher binding energies. On the 2 ML of Ni film, there is an intense peak at 1 eV binding energy. The transition metal film appears to assume a more noble metal-like character in that a well-defined d band is evident that is separated from the Fermi edge.[11,12] Similar behavior, with a loss of intensity at the Fermi level and the growth of a peak at higher binding energies, has been observed for thin films of Pd on W(001).[25] Perhaps the redistribution of charge, as indicated by the discrete band below the Fermi level, allows for a different interaction between the metal and the adsorbate that might destabilize the C−S bond. Based on a thermochemical analysis, Rodriguez predicted that the C−S bond scission reaction would become more exothermic and that the S−H bond scission reaction would become less

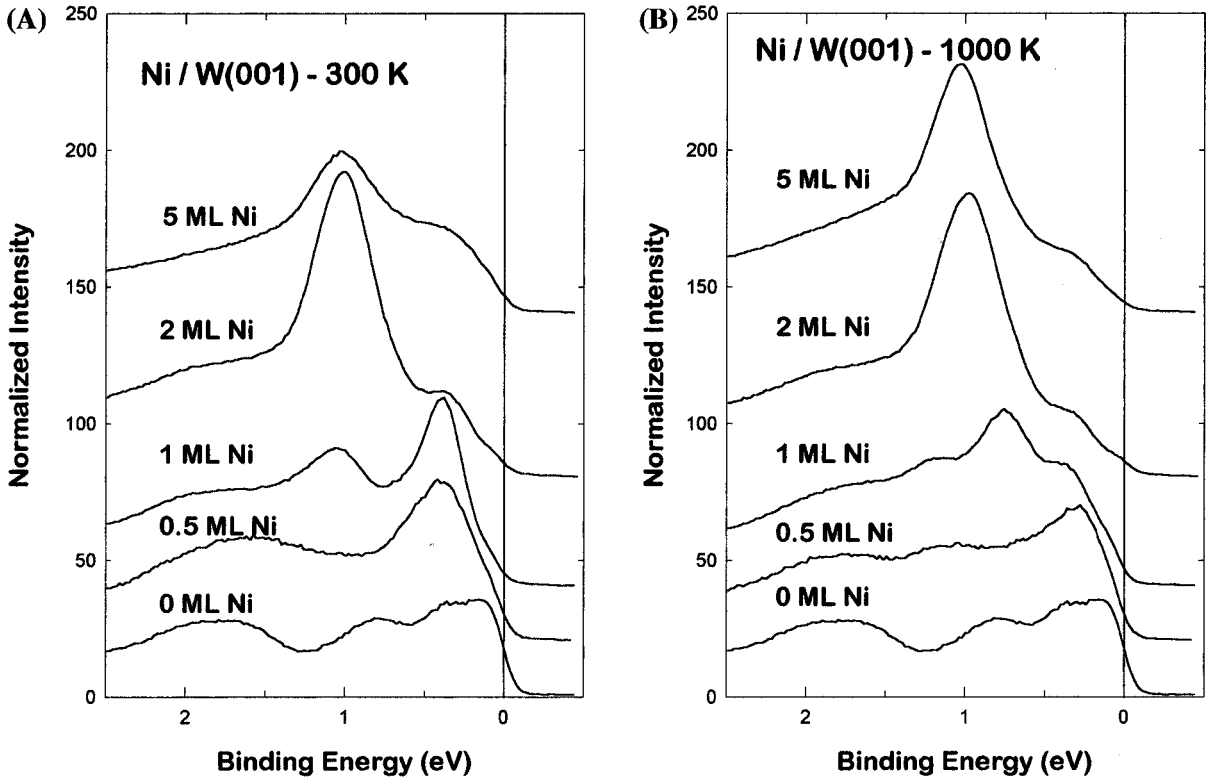

Figure 12. Valence band photoemission spectra from W(001) covered with various amounts of Ni: (A) annealed to 300 K; (B) annealed to 1000 K. The photon energy was 70 eV, and emission was normal to the surface.

exothermic as the substrate was changed from metals on the left-hand side of the periodic table to metals on the right-hand side.[26] These predictions are consistent with what is observed for CH_3SH on the strained Ni films compared to clean W(001). It can be seen in Figure 12A that there is a suppression of the peak at 1 eV for an unannealed, 5 ML film where the strain is presumably relieved through dislocations and defects as the thickness grows. The suppression of the peak at 1 eV is consistent with the decrease in methane selectivity (Figure 2) and the increase in the methane desorption temperature (Figure 4) that are observed on the unannealed thick films. If the substrate is annealed, as in Figure 12B, the peak at 1 eV increases in intensity compared to the unannealed film, and the methane selectivity and desorption temperature are similar to what was observed on the 2 ML film.

The decomposition of CH_3SH behaves very differently on Ni-covered W(001) than it does on Co-covered Mo(110).[15] On Mo(110), 50% of the CH_3SH totally decomposes and this percentage stays the same as the surface is covered with Co. The only significant change is a transition from methyl desorption to methane desorption as the Co coverage is increased. As shown above, on W(001) the amount of total decomposition falls dramatically as the surface is covered with Ni. There are several obvious differences between the two systems. The reactivity of CH_3SH on Co and Mo is very similar as shown by the decomposition behavior on clean Mo(110) and thick/bulk Co. Ni and W, on the other hand, lie at the extremes in terms of their relative reactivity toward CH_3SH decomposition. Decomposition on Ni strongly favors methane formation, whereas decomposition on W favors total decomposition. If the systems simply followed a linear transition from substrate behavior to admetal behavior, one would anticipate a change on Ni/W and not on Co/Mo. Furthermore, the metal film is much more strained on the W(001) surface compared to the Mo(110) surface. The Co−Co nearest-neighbor distance in the first layer is 2.73 Å on Mo(110) compared to 2.51 Å on Co(0001). The Ni−Ni nearest-neighbor distance in the first layer is 3.15 Å on W(001) compared to 2.49 Å on Ni(001). In addition, two strained layers of Ni can be grown on the W(001) surface and only one layer of Co can be grown on Mo(110). At higher coverages, the Co reconstructs into a Co(0001) structure.[27] If the properties of the film are altered by the film's structure then Ni/W(001) would be expected to show a bigger effect than Co/Mo(110). An investigation using Co on W(001) or Ni on W(110) would help sort out the effects due to the identity of the admetal and the structure of the film.

Summary

Thin films of Ni enhance the selectivity for methane formation during the decomposition of CH_3SH on W(001). On a 2 ML film, >85% of the CH_3SH produces methane. This is the largest selectivity for methane formation observed on a metal surface under ultrahigh vacuum conditions. The increase in selectivity is accompanied by a decrease in the methane desorption temperature. Both results are attributed to a destabilization of the C−S bond on the Ni film. The decrease in the C−S bond cleavage temperature allows the methane formation reaction to compete more effectively with H_2 desorption and methyl decomposition. The most pronounced effects are on the strained, homogeneous Ni films. The change in selectivity is attributed to an alteration of the Ni electronic structure due to the lattice strain.

Acknowledgment. The author thanks Paul Lyman for providing the valence band photoemission spectra and D. R. Huntley for helpful discussions during the preparation of the manuscript. Research was sponsored by the Division of Chemical Sciences, Office of Basic Energy Sciences, U.S. Department of Energy at Oak Ridge National Laboratory, managed by Lockheed Martin Energy Research Corp. under Contract Number DE-AC05-96OR22464. The National Syn-

chrotron Light Source at Brookhaven National Laboratory is supported by the Division of Chemical Sciences and Division of Material Sciences of the U. S. Department of Energy under Contract DE-AC02-76CH00016.

References and Notes

(1) Mullins, D. R.; Lyman, P. F. *J. Phys. Chem.* **1993**, *97*, 9226.
(2) Castro, M. E.; Ahkter, S.; Golchet , A.; White, J. M. ; Sahin, T. *Langmuir* **1991**, *7*, 126.
(3) Rufael, T. S.; Huntley, D. R.; Mullins, D. R.; Gland, J. L. *J. Phys. Chem.* **1995**, *99*, 11472.
(4) Huntley, D. R. *J. Phys. Chem.* **1989**, *93*, 6156.
(5) Rufael, T. S.; Koestner, R. J.; Kollin, E. B.; Salmeron, M.; Gland, J. L. *Surf. Sci.* **1993**, *297*, 272.
(6) Sexton, B. A.; Nyberg, G. L. *Surf. Sci.* **1986**, *165*, 251.
(7) Albert, M. R.; Lu, J. P.; Bernasek, S. L.; Cameron, S. D.; Gland, J. L. *Surf. Sci.* **1988**, *206*, 348.
(8) Mullins, D. R.; Lyman, P. F. *J. Phys. Chem.* **1993**, *97*, 12008.
(9) Wiegand, B. C. ; Uvdal, P.; Friend, C. M. *Surf. Sci.* **1992**, *279*, 105.
(10) Benziger, J. B.; Preston, R. E. *J. Phys. Chem.* **1985**, *89*, 5002.
(11) Campbell, C. T. *Annu. Rev. Phys. Chem.* **1990**, *41*, 775.
(12) Rodriguez, J. A.; Goodman, D. W. *J. Phys. Chem.* **1991**, *95*, 4196.
(13) Pecoraro, T. A.; Chianelli, R. R. *J. Catal.* **1981**, *67*, 430.
(14) Overbury, S. H.; Lyman, P. F.; Mullins, D. R.; Shinn, N. D. *Surf. Sci.* **1995**, *339*, 68.
(15) Chen, D. A.; Friend, C. M.; Xu, H. *Langmuir* **1996**, *12*, 1528.
(16) Berlowitz, P. J.; Goodman, D. W. *Surf. Sci.* **1987**, *187*, 463.
(17) Huntley, D. R. *J. Phys. Chem.* **1993**, *97*, 12008.
(18) *Selected Mass Spectral Data*; Thermodynamics Research Center: College Station, Texas, 1982.
(19) Mullins, D. R.; Lyman, P. F. *J. Phys. Chem.* **1995**, *99*, 5548.
(20) These peak positions, 283.2, 284.7, and 286.2 eV, were previously reported as 282.3, 283.8, and 285.6 eV.[1,18] This discrepancy has been traced to an error in analyzer calibration in the earlier work, and the present values are more accurate.
(21) Overbury, S. H.; Mullins, D. R. *Surf. Sci.* **1996**, *369*, 231.
(22) Mullins, D. R.; Tang, T.; Chen, X.; Shneerson, V.; Saldin, D. K.; Tysoe, W. T. *Surf. Sci.*, in press.
(23) Mullins, D. R.; Huntley, D. R.; Tang, T.; Saldin, D. K.; Tysoe, W. T. *Surf. Sci.*, in press.
(24) Mullins, D. R.; Lyman, P. L. *Langmuir*, in press.
(25) Grahm, G. W. *J. Vac. Sci. Technol. A* **1986**, *4*, 760.
(26) Rodriguez, J. A. *Surf. Sci.* **1992**, *278*, 326.
(27) Chen, D. A.; Friend, C. M. *Surf. Sci.*, submitted for publication.